

PAPER *Special Section of Papers Selected from the 8th Digital Signal Processing Symposium*

Improved Contextual Classifiers of Multispectral Image Data*

Takashi WATANABE†, *Member*, Hitoshi SUZUKI††, Sumio TANBA†, *Nonmembers*
and Ryuzo YOKOYAMA†, *Member*

SUMMARY Contextual classification of multispectral image data in remote sensing is discussed and concretely two improved contextual classifiers are proposed. The first is the extended adaptive classifier which partitions an image successively into homogeneously distributed square regions and applies a collective classification decision to each region. The second is the accelerated probabilistic relaxation which updates a classification result fast by adopting a pixelwise stopping rule. The evaluation experiment with a pseudo LANDSAT multispectral image shows that the proposed methods give higher classification accuracies than the compound decision method known as a standard contextual classifier.

key words: *contextual classification, multispectral image, remote sensing, probabilistic relaxation*

1. Introduction

In remote sensing, classification of multispectral image data has been widely used as a powerful means to extract various kinds of informations concerning the earth environment [6]. Classification is based on reflection spectrum characteristics of objects in a multispectral image. Pixelwise classifiers, such as the maximum likelihood method, that perform classification on a single pixel base have been widely used so far, but they cannot attain a higher classification accuracy. Therefore, contextual classifiers that utilize spatial contextual informations among neighboring pixels have attracted attention and have been studied [2], [5], [7], [9].

In this paper, we propose two improved contextual classifiers. The first is the extended adaptive classifier which is an improved method of the adaptive classifier [8]. In the method, an image is partitioned successively into homogeneously distributed regions and a collective classification decision is applied to each region. A region has a square shape and it is repeatedly partitioned into four square regions of the same size until the resulting regions are homogeneous. When a successful classification is not realized even at a 2×2 (pixels) square region, a consecutive procedure

of three classifications is applied. They are a classification using four-pixels regions, a classification using three-pixels regions and a pixelwise classification.

The second is the accelerated probabilistic relaxation. A probabilistic relaxation [3], [4] is an iterative processing which updates a classification result of each pixel so that it is consistent with the context of neighborhood. The traditional probabilistic relaxations may attain a high classification accuracy, but they have two serious problems. One is that they are heavy time consumers and the other is that their updating effects are limited only at the early iterations. To overcome the problems, we propose an acceleration method of probabilistic relaxations that uses a pixelwise stopping rule in iterations. Introducing this rule, we can drastically reduce a CPU time of relaxation processing and simultaneously avoid the obstacle that a classification accuracy degenerates as an iteration goes on.

We have made an experiment with a pseudo LANDSAT multispectral image to evaluate the proposed methods objectively. Consequently, both the proposed methods gave higher classification accuracies than the compound decision method [1], [5] known as a standard method of statistical contextual classification. The compound decision is such a method as minimizes an expected loss of classification under utilizing the neighboring pixels and the details are given in Refs. [9] and [10]. Moreover, it is shown that the pixelwise stopping rule made a drastic acceleration of relaxation processing.

2. Extended Adaptive Classification

In a multispectral image, let us denote the set of pattern classes by $\Omega = \{1, 2, \dots, m\}$ and a feature vector of pixel by x , where m is the number of classes.

In the adaptive classifier [8], the image is partitioned successively into homogeneously distributed regions and each region is classified collectively into a single class. Each partitioned region has a square shape of $2^k \times 2^k$ pixels ($k \geq 1$) and it is repeatedly partitioned into four square regions of the same size until the resulting regions are homogeneous. If a successful classification is not realized even at a 2×2 square region, the maximum likelihood method of

Manuscript received December 20, 1993.

Manuscript revised April 13, 1994.

† The authors are with the Faculty of Engineering, Iwate University, Morioka-shi, 020 Japan.

†† The author is with the Product Engineering Department, NEC Corporation, Fuchu-shi, 183 Japan.

* This paper was presented at ISPACS '93.

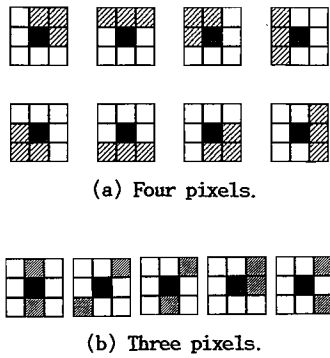


Fig. 1 Block patterns of four pixels and three pixels in extended adaptive classifier.

pixelwise classification is applied.

The adaptive classifier has the problem that most of the pixels at the boundary and line part in the image are classified pixelwise and its classification accuracy may not be so high. To improve this, we present a new classifier, called the extended adaptive classifier.

The procedure of the extended adaptive classifier is shown in the following.

step 1: Partition the image into initial square regions of a specified size.

step 2: Choose a square region and apply the two judgments, described later, to the region. If both the judgments return YES's, classify all the pixels in the region to the candidate class. If not so, partition the region into four squares of the same size.

step 3: Iterate step 2 as long as there remains an unclassified square region.

step 4: If the partitioning proceeds down to a pixel, classify the pixel as follows.

(4. 1) Among eight kinds of four-pixels regions with the pixel as the center, as are shown in Fig. 1(a), select one with the minimum variance and apply the two judgments, described below, to it. If both the judgments return YES's, classify the pixel to the candidate class. If not so, go to (4. 2).

(4. 2) Among arbitrary three-pixels regions with the pixel as the center, (there are 28 such patterns as are reduced to the prototypes shown in Fig. 1(b)), select one with the minimum variance and apply the two judgments to it. If both the judgments return YES's, classify the pixel to the candidate class. If not so, classify the pixel pixelwise by the maximum likelihood method.

The following two judgments are used to classify each region.

[Judgment 1] (judgment by mean vector)

Let M be the number of pixels in the region and \bar{x} be the mean vector of pixels $\{x_1, x_2, \dots, x_M\}$ in the region. The distance like the Maharanobis one between \bar{x} and μ_ω is defined by

$$d_M(\omega) = M (\bar{x} - \mu_\omega)^T S_\omega^{-1} (\bar{x} - \mu_\omega), \quad (1)$$

where μ_ω is the mean vector for class $\omega \in \Omega$ and S_ω is the covariance matrix for class ω . We select the class ω that minimizes

$$d_M(\omega) + \log|S_\omega| \quad (2)$$

in Ω . If ω satisfies

$$d_M(\omega) \leq r_M, \quad (3)$$

then YES is returned and ω is set as the candidate class, where r_M is a threshold. If not so, NO is returned. [Judgment 2] (judgment by sum)

For the candidate class ω in the judgment 1, the sum of the Maharanobis distances between x_j and μ_ω is defined by

$$D_M(\omega) = \sum_{j=1}^M (x_j - \mu_\omega)^T S_\omega^{-1} (x_j - \mu_\omega). \quad (4)$$

We select the class ω that minimizes

$$D_M(\omega) + \log|S_\omega| \quad (5)$$

in Ω . If ω satisfies

$$D_M(\omega) \leq t_M, \quad (6)$$

then YES is returned, where t_M is a threshold. If not so, NO is returned.

Consider the hypothesis H: "All pixels in a region to be classified are random samples from the ensemble with normal distribution $N(\mu_\omega, S_\omega)$." Under the hypothesis H, $d_M(\omega)$ and $D_M(\omega)$ follow χ^2 -distributions with degrees of freedom n and nM , respectively. Then, using the significance levels (upper probabilities) α_M and β_M , we can define the thresholds r_M and t_M from the relations

$$\text{Prob}[d_M(\omega) > r_M | H] = \alpha_M \quad (7)$$

$$\text{Prob}[D_M(\omega) > t_M | H] = \beta_M, \quad (8)$$

where the suitable values of α_M and β_M must be determined based on experiments.

3. Accelerated Probabilistic Relaxation

Let x_i be a feature vector of i -th pixel and $s_i(\omega)$ be the likelihood of x_i belonging to class ω . A membership vector $s_i = [s_i(1), s_i(2), \dots, s_i(m)]$ satisfies the following two relations

$$0 \leq s_i(\omega) \leq 1 \quad (9)$$

$$\sum_{\omega \in \Omega} s_i(\omega) = 1. \quad (10)$$

In a probabilistic relaxation, a vector s_i is updated to be consistent with the context of neighborhood. In this paper, we discuss the following two relaxations to update a vector s_i^k , where s_i^k denotes the altered vector of s_i at the k -th iteration.

[Rosenfeld's Relaxation] [3]

We denote by θ_i the true class membership of i -th pixel

x_i and consider it as a random variable. Then, s_i^k is updated by

$$s_i^{k+1}(\omega) = \frac{s_i^k(\omega)(1+q_i^k(\omega))}{\sum_{\omega \in \Omega} s_i^k(\omega)(1+q_i^k(\omega))} \quad (11)$$

$$q_i^k = \sum_{j \in N_i} d_{ij}(\omega) \sum_{\omega' \in \Omega} r_{ij}(\omega, \omega') s_j^k(\omega') \quad (12)$$

$$r_{ij}(\omega, \omega') = c \log\{p(\theta_i = \omega | \theta_j = \omega') / p(\theta_i = \omega)\}, \quad (13)$$

where N_i is the set of neighbor pixels for i -th pixel. $p(\theta_i = \omega)$ is the a priori probability that i -th pixel takes class ω and $p(\theta_i = \omega | \theta_j = \omega')$ is the conditional probability that i -th pixel takes class ω , given that j -th neighbor pixel takes class ω' . d_{ij} is a nonnegative weight and c is a constant value. The value of r_{ij} is clipped in the range $[-1, 1]$ when it exceeds the range. [Peleg's Relaxation] [4]

s_i^k is updated by

$$s_i^{k+1}(\omega) = \sum_{j \in N_i} c_j \frac{s_i^k(\omega) Q_{ij}^k(\omega)}{\sum_{\omega \in \Omega} s_i^k(\omega) Q_{ij}^k(\omega)} \quad (14)$$

$$Q_{ij}^k(\omega) = \sum_{\omega' \in \Omega} r_{ij}(\omega, \omega') s_j^k(\omega') \quad (15)$$

$$r_{ij}(\omega, \omega') = p(\theta_i = \omega | \theta_j = \omega') / p(\theta_i = \omega), \quad (16)$$

where c_j is a nonnegative weight. In this case, $r_{ij}(\omega, \omega')$ takes a value in the range $[0, \infty)$.

The initial vector s_i^0 is chosen by

$$s_i^0(\omega) = p(\theta_i = \omega | x_i), \quad (17)$$

where $p(\theta_i = \omega | x_i)$ is the posteriori probability that i -th pixel takes class ω , given that its feature vector is x_i . The classification decision of x_i at the k -th iteration results in the selection of the class $\omega \in \Omega$ maximizing $s_i^k(\omega)$.

The above traditional relaxations may attain a higher classification accuracy than pixelwise classifiers, but they have two serious problems. One is that they are heavy time consumers and the other is that their updating effects are limited only at the early iterations. The latter is prominent in the Peleg's relaxation, and this may throw a question to the validity of convergence in relaxation. To overcome these problems, we introduce a pixelwise stopping rule given as follows. [Pixelwise Stopping Rule]

We assume that at the k -th iteration the most probable class of x_i is ω , namely,

$$s_i^k(\omega) = \max_{\omega' \in \Omega} \{s_i^k(\omega')\}. \quad (18)$$

If, at the next $(k+1)$ -th iteration, we have the following two relations

$$s_i^{k+1}(\omega) = \max_{\omega' \in \Omega} \{s_i^{k+1}(\omega')\} > s_i^k(\omega) \quad (19)$$

$$s_i^{k+1}(\omega') \leq s_i^k(\omega') \quad (\omega' \neq \omega), \quad (20)$$

then we rewrite the vector s_i^{k+1} as follows:

$$s_i^{k+1}(\omega') = \begin{cases} 1 & (\omega' = \omega) \\ 0 & (\omega' \neq \omega). \end{cases} \quad (21)$$

The above rewriting is justified because Eqs. (19) and (20) mean that classifying x_i to class ω is supported by the neighborhood and the likelihood $s_i(\omega')$ would be increased only for $\omega' = \omega$ through the following iterations. Therefore, the rewritten s_i^{k+1} should not be altered afterwards, that is, we assume the following relations

$$s_i^{k+1}(\omega') = s_i^{k+2}(\omega') = \dots \quad (22)$$

for all $\omega' \in \Omega$.

The stopping rule may reduce a total processing time of relaxation considerably, because pixels to be updated are monotonously decreased as an iteration goes on. Also the validity problem of convergence may be improved by the stopping rule. The reason is as follows. As the exact estimation of $r_{ij}(\omega, \omega')$ is difficult, an update introduces a little uncertainty unavoidably. Therefore, a relaxation brings simultaneously an improvement of contextual adjustment and a diffusion of uncertainty, and consequently the classification accuracy fluctuates as an iteration goes on. At the early iterations, the class supported by the neighborhood can be considered to be reliable, because it is less blotted in uncertainty. Therefore, fixing the vector s_i of the supported pixel in early stages, we can suppress the diffusion of uncertainty and consequently prevent the degeneration of classification accuracy in relaxation processing.

4. Experiment and Discussion

4.1 Image Data Used in Experiment

As long as an actual image data is used as a test data in evaluation experiment of classifiers, it is difficult to get an objective evaluation. The reason is that it is hard to specify training areas appropriately in the image and a subjective specification through human recognition is inevitable. Therefore, we used a pseudo LANDSAT MSS image as a test data in the experiment.

The pseudo image data was constructed as follows. First, we partitioned the 1/25,000 map (Morioka) of the National Geographical Institute into meshes of 50 meters' step and made a landuse map (6.4 km \times 6.4 km, 128 \times 128 pixels) by specifying the landcover class of each mesh, where there are such eight classes as residential area, urban area, road, bare soil, rice field, field, forest and water area. Second, using the actual LANDSAT MSS image data containing the corresponding areas (photographically taken

August 6, 1983, with bands 5 and 6), we estimated the average vector μ_ω and the covariance matrix S_ω for each class ω . For each mesh of the landuse map, we generated the two-dimensional random numbers following the normal distribution $N(\mu_\omega, S_\omega)$ and obtained the pseudo LANDSAT MSS image. This pseudo image was originally used in Ref. [9]. If a reader want to get more information about it, he should go into the reference.

We used the following definition to represent a classification accuracy:

$$\begin{aligned} & \text{(class recognition rate)} \\ &= \frac{\text{(number of correctly recognized pixels)}}{\text{(total number of pixels in the class)}} \end{aligned}$$

Class mean recognition rate is the simple average of class recognition rates and total recognition rate is the weighted average of them with class area ratios.

4.2 Results of Extended Adaptive Classification

In the extended adaptive classification, a pixel classified by utilizing the neighboring pixels is called a blocked pixel and the ratio of blocked pixels to all the pixels is called a blocking rate. Figure 2 shows a relationship between significance level and blocking rate, where the curve marked with $n \times n$ pixels (n pixels) indicates the ratio of the blocked pixels that are classified by utilizing the regions of the size of $n \times n$ pixels (n pixels) and more pixels. From this, we can see that the number of pixelwise classified pixels increases as a significance level comes near to one. Especially, it should be noted that the ratio of the pixels classified with the regions of four pixels and three pixels occupies 30 to 50 percent of all the pixels at the significance level from 0.1 to 0.25. These pixels have been classified pixelwise in the traditional adaptive classifier.

Figure 3 shows a relationship between significance level and total recognition rate. The curve marked with 2×2 pixels corresponds to the traditional adaptive classifier and the curve marked with 3 pixels does to the extended adaptive classifier. The curve marked with 4 pixels shows the total recognition rate of the extended adaptive classifier when it uses only the four-pixels regions without employing the three-pixels regions in step 4. From this, we can see that the total recognition rate got the maximum value at the significance level of 0.25 and that the extended adaptive classifier improved about five percent of recognition rate compared with the traditional adaptive classifier.

The processing time of the extended adaptive classifier increased a little than the traditional one. Thus, we can conclude that the extended adaptive classifier makes a more adaptive classification than the traditional classifier and gives a fair improvement on

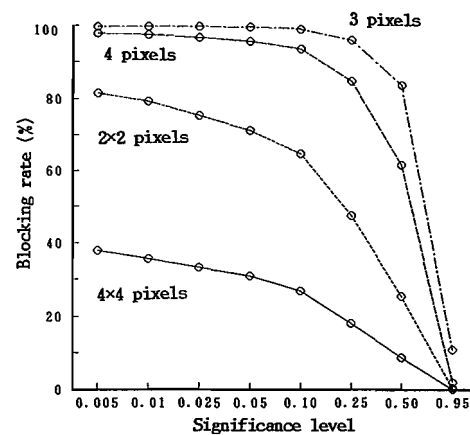


Fig. 2 Blocking rate in extended adaptive classifier.

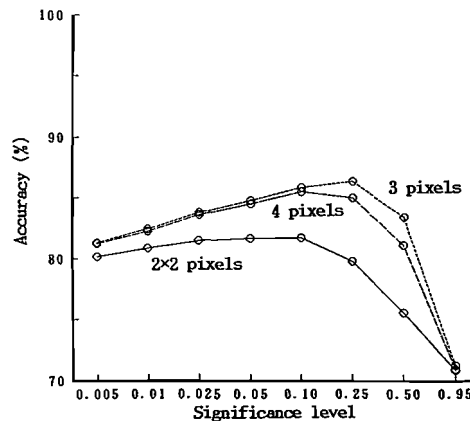


Fig. 3 Classification accuracies of adaptive classifier and extended adaptive classifier.

classification accuracy.

4.3 Results of Probabilistic Relaxations

The neighborhood type was of 3×3 pixels and $d_{ij} = c_j = 1/8$ were chosen in the experiment. c was set to 0.2 because it gave the highest recognition rate among some tested values. The values of $p(\theta_i = \omega)$ and $p(\theta_i = \omega | \theta_j = \omega')$ were newly estimated at each iteration from the classification result, where each pixel was classified to the class ω maximizing $s_i^k(\omega)$. Especially, at the first iteration $k=0$, the classification result with the Bayesian decision was used, where the value of $p(\theta_i = \omega)$ was estimated from the classification result with the maximum likelihood method.

Figure 4 shows the total recognition rates of the Rosenfeld's relaxation, where the *modified case* indicates the relaxation using the stopping rule and the *original case* does the relaxation without the stopping rule. In the figure $c=0.2$ was selected and for the different values of c the original case did not surpass the modified case. Similarly, Fig. 5 shows the total recognition rates of the Peleg's relaxation. From these,

we can see that the stopping rule dissolved the problem that the classification accuracy degenerates as an iteration goes on.

Figure 6 shows the CPU time consumed in the Rosenfeld's relaxation and Fig. 7 does that in the Peleg's relaxation. From these results, we can see that the stopping rule accelerated the relaxation processing dramatically.

Lastly, we show the classification accuracies of the tested classifiers in Table 1, where for each relaxation the best of accuracies at iterations is filled in. In the table, the classifiers of the extended adaptive classification and the two accelerated relaxations got higher

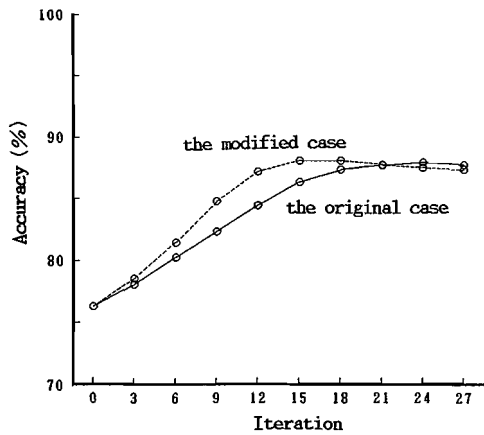


Fig. 4 Classification accuracy of Rosenfeld's relaxation.

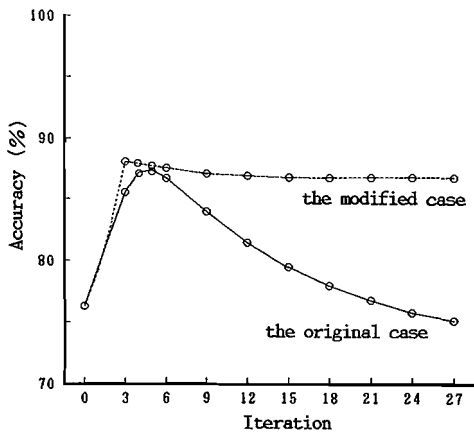


Fig. 5 Classification accuracy of Peleg's relaxation.

classification accuracies than the compound decision method. The extended adaptive classification showed a little lower accuracy than both of the accelerated relaxations, but the former is superior to the latter in CPU time and memory storage. Therefore, it can be said that in practical use the extended adaptive classification is more convenient than the accelerated relaxations.

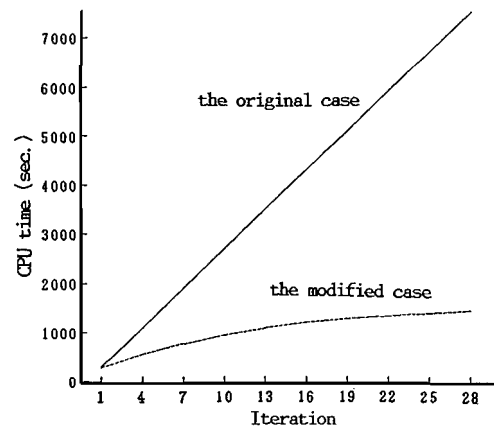


Fig. 6 CPU time used in Rosenfeld's relaxation.

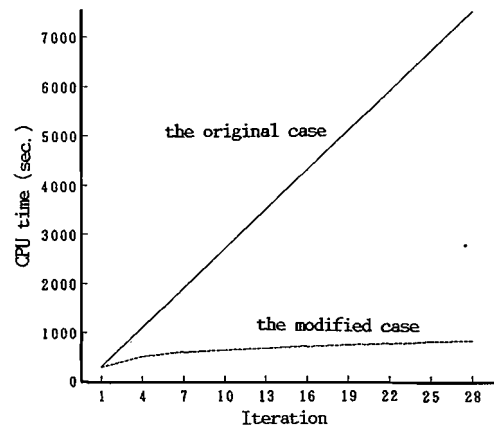


Fig. 7 CPU time used in Peleg's relaxation.

Table 1 Classification accuracies of the tested classifiers.

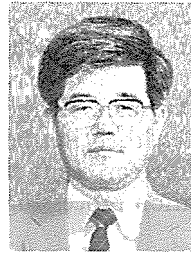
| | Maximum Likelihood | Bayes Decision | Compound Decision | Adaptive Classifier | Extended Adaptive Classifier | Rosenfeld Relaxation | Accel. Rosenfeld Relaxation | Peleg Relaxation | Accel. Peleg Relaxation |
|-----------------------------|--------------------|----------------|-------------------|---------------------|------------------------------|----------------------|-----------------------------|------------------|-------------------------|
| Class-Mean Recognition Rate | 73.64 | 64.91 | 84.33 | 81.45 | 86.15 | 87.66 | 88.83 | 88.52 | 87.74 |
| Total Recognition Rate | 70.83 | 78.92 | 84.99 | 81.79 | 86.43 | 87.96 | 88.10 | 87.52 | 88.19 |

5. Conclusion

In this paper, we discussed the contextual classifiers that utilize the spatial-contextual informations among neighbor pixels to get a higher classification accuracy than pixelwise classifiers. Actually, we proposed the two contextual classifiers of the extended adaptive classification and the accelerated probabilistic relaxation. To evaluate the proposed methods, we have made an experiment using a pseudo LANDSAT multispectral image data. Consequently, the experimental results showed that both the proposed methods got higher classification accuracies than the compound decision method known as a standard contextual classifier. Also, compared with the traditional probabilistic relaxations, the accelerated probabilistic relaxations could reduce the CPU time dramatically. Therefore, it is expected that the proposed methods would be widely used as convenient contextual classifiers.

References

- [1] Welch, J. R. and Salter, K. G., "A context algorithm and image interpretation," *IEEE Trans. Syst. Man. & Cybern.*, vol. SMC-1, no. 1, pp. 24-30, 1971.
- [2] Kettigh, R. L. and Landgrebe, D. A., "Classification of multispectral image data by extraction and classification of homogeneous objects," *IEEE Trans. Geosci. Electronics*, vol. GE-14, pp. 19-26, 1976.
- [3] Eklund, J. O., Yamamoto, H. and Rosenfeld, A., "A relaxation method for multispectral pixel classification," *IEEE Trans. Pattern Anal. & Mach. Intell.*, vol. PAMI-2, no. 1, pp. 72-75, 1980.
- [4] Peleg, S., "A new probabilistic relaxation scheme," *IEEE Trans. Pattern Anal. & Mach. Intell.*, vol. PAMI-2, no. 4, pp. 362-369, 1980.
- [5] Swain, P. H., Varclleman, S. B. and Tilton, J. C., "Contextual classification of multispectral image data," *Pattern Recognition*, vol. 13, no. 6, pp.429-441, 1981.
- [6] Swain, P. H., "Advanced interpretation techniques for earth data information system," *Proc. IEEE*, vol. 73, no. 6, pp.1031-1039, 1985.
- [7] Harris, R., "Contextual classification postprocessing of LANDSAT data using a probabilistic relaxation model," *Int. J. Remote Sensing*, vol. 6, no. 6, pp. 847-866, 1985.
- [8] Takahashi, T., Fujimura, S. and Toyota, H., "Adaptive classification of multispectral images using local uniformity," *Trans. of the Society of Instrument & Control Engineers*, vol. 21, no. 2, pp. 164-171, 1985.
- [9] Watanabe, T. and Suzuki, H., "An experimental evaluation of classifiers using spatial context for multispectral images," *Systems and Computers in Japan*, vol. 19, no. 4, pp. 33-47, 1988.
- [10] Watanabe, T., Suzuki, H., Tanba, S. and Yokoyama, R., "Improved contextual classifiers of multispectral image data," *Proceedings of International Workshop on Intelligent Signal Processing and Communication Systems (ISPACS'93)*, pp. 303-308, 1993.



Takashi Watanabe was born in Yamanashi Prefecture, Japan on April 1, 1947. He received B.E., M.E. and Ph.D. degrees from Tohoku University, Japan, in 1969, 1971 and 1980, respectively. From 1972 to 1976, he had worked for Hitachi, Ltd., Japan. Since 1980, he has been with Iwate University, Japan, where he is presently a Professor in the Department of Computer and Information Science, Faculty of Engineering. His research interest includes image processing, pattern recognition and remote sensing. He is a member of the Information Processing Society of Japan, the Remote Sensing Society of Japan and the Society of Instrument and Control Engineers of Japan.



Hitoshi Suzuki was born in Aomori Prefecture, Japan on June 30, 1962. He received B.E. and M.E. degrees in computer science from Iwate University, Japan, in 1985 and 1987, respectively. Since 1987, he works for NEC Corporation, Japan and his current position is the assistant manager for planning of engineering workstations. His research interest includes image processing, pattern recognition and remote sensing. He is a member of the Information Processing Society of Japan.



Sumio Tanba was born in Hokkaido Prefecture, Japan on Decemere 23, 1959. He received B.E. and M.E. degrees in computer science from Iwate University, Japan, in 1983 and 1985, respectively. Since 1985, he has been a research associate in the Department of Computer and Information Science, Faculty of Engineering, Iwate University. His research interest includes remote sensing and image processing. He is a member of IEEE, the Remote Sensing Society of Japan and the Information Processing Society of Japan.



Ryuzo Yokoyama was born in Pusan, Korea on September 14, 1939. He received B.E., M.E. and Ph.D. degrees from Tohoku University, Japan, in 1964, in 1966 and from University of Rochester, U.S.A., in 1969, respectively. From 1970 to 1972 he had been a research associate at Tohoku University. Since 1972, he has been with Iwate University, Japan, where he is presently a Professor in the Department of Computer and Information Science, Faculty of Engineering. His research interest includes remote sensing, system science and image processing, etc.. He is a member of IEEE, the Information Processing Society of Japan, the Remote Sensing Society of Japan and the Society of Instrument and Control Engineers of Japan.